# Electrical measurements on fused quartz under shock compression

Ken-ichi Kondo and Akira Sawaoka
*Research Laboratory of Engineering Materials, Tokyo Institute of Technology, Nagatsuta, Midori, Yokohama 227, Japan*

Thomas J. Ahrens
*Seismological Laboratory, California Institute of Technology, Pasadena, California 91125*

(Received 28 January 1981; accepted for publication 23 April 1981)

The resistivities of specimens of $SiO_2$ (fused quartz) singly and doubly shocked in the 10–45 and 27–90 GPa ranges, respectively, demonstrate a marked decrease from values of ~10–0.1 Ω·m at a single-shock pressure of ~40 and a double-shock pressure of ~74 GPa. These states correspond to calculated shock temperatures of ~3300 and ~3600 K, respectively. At shock pressures below 36 GPa the measured resistivity versus calculated shock temperature agrees closely with ambient-pressure and high-temperature resistivity data. This suggests that the ionic conduction mechanisms inferred to control electrical properties at ambient pressure also act under shock-induced high temperatures in quartz and the presumed high-pressure phase, stishovite into which fused quartz appears to transform above 20 GPa. At 36–40 GPa the rapid decrease in resistivity by a factor of $10^2$ suggests a further transformation to an unknown phase which may correspond to the onset of melting. The existing pressure-density Hugoniot data do not demonstrate any anomalous density change associated with this phase change.

PACS numbers: 64.90. + b, 62.50. + p, 66.30.Dn, 77.90. + k

## I. INTRODUCTION

Although the shock wave equation of state of single-crystal density[1,2] and porous quartz[3] and fused $SiO_2$ (Refs. 1, 3, and 4) have been studied over a wide range of dynamic pressures, previous studies of the electrical properties of quartz have been limited to studies of single-crystal quartz[5] as these pertain to the use of this material as a shock transducer material. Wackerle's[1] study of the Hugoniot equation of state of single and fused quartz demonstrated both high dynamic yield strength and the onset of a shock-induced phase change. McQueen *et al.*[6] first suggested that the phase change in both materials was due to the formation of rutile-structured high-pressure polymorph, stishovite, which was later recovered from laboratory shock loaded $SiO_2$[7]. Also the kinetics of the quartz-to-stishovite transition and its effect on wave propagation in the range of shock pressures 14–40 GPa, in which both quartz and stishovite are thought to be present, the so-called mixed phase region of $SiO_2$, have been investigated during shock compression by using in-material particle velocity and shock stress gauges[8]. Other physical properties of $SiO_2$ under shock compression have not yet been explored. We have performed measurements of electrical resistivity under dynamic high-pressure and shock-induced electromotive force on fused quartz specimens which were singly and doubly shocked into the stress range of 10–90 GPa upon impact with projectiles launched with a two-stage light-gas gun. The resulting data are discussed in light of our knowledge of the electrical properties of dielectrics and their relation to the previous equation of state studies.

## II. EXPERIMENTAL

Shock experiments were conducted using a two-stage light-gas gun (HS-2, Tokyo Institute of Technology).[9] The sample assembly (Fig. 1) was impacted by a copper or tungsten flyer plate affixed to a 20-mm-diam. high-density polyethylene sabot. Both resistivity and shock-induced polarization measurements were carried out in longitudinal geometry of Fig. 1. Two specimens were attached to independent copper backing electrodes (3–4 mm in diameter and 5 mm in height) and mounted on a common delay buffer plate which was placed on the target driver plate. One of the specimens was used for the resistivity measurement and the other for the polarization measurement. Six coaxial pin contactors were placed around the specimens; two of them were to provide redundant trigger signals for single-sweep oscilloscopes and the remaining four to observe flyer-plate tilt.[10] Flyer-plate tilts were less than 0.5°. Using an acrylic case, the specimens were surrounded with 99.99% He at 1 atm, so that ionized gas species did not provide a short-circuit path for the resistivity measurement.

The fused quartz, of stock commercial grade (Amersil Corp.), had a uniform initial density of 2.204 $Mg/m^3$. The disc-shaped specimens were polished to provide good electrical contact with the target driver plate and the backing electrode.

A charged-capacitor method[11–13] was used for measuring the sample electrical resistivity. With this circuit, current

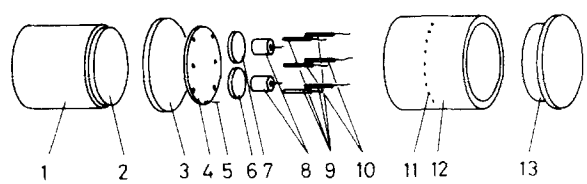


FIG. 1. Schematic diagram of sample assembly for measuring electrical resistivity and polarization under shock compression. 1: polyethelene sabot (20 mm in diameter), 2: flyer plate, 3: target driver plate, 4: delay buffer plate, 5: ground lead, 6: specimen for resistivity measurement, 7: specimen for polarization measurement, 8: backing electrode, 9: tilt pins, 10: trigger pins, 11: holes for electric leads, 12: acrylic case, and 13: lid.




0021-8979/81/085084-06$01.10

flows from the target driver plate, via the sample, to the backing electrode. For polarization measurements, the specimen was considered to be a current source which is terminated with 50 $\Omega$ to match the cable impedance. The effective area for the reflected shock state was estimated by assuming that rarefaction wave from a free surface of the specimen propagates along a direction of 45° from the edge of the electrode.

The impedance match method was used to determine both the initial and reflected shock states in the specimen using the Hugoniot data of McQueen[14] and Wackerle,[1] for copper, tungsten, and fused quartz. In this paper, both reflected Hugoniot and isentropic state were approximated using the principal Hugoniot curve.

Shock temperatures were estimated on the basis of the following equations:

$$\tfrac{1}{2}P_H(V_{00} - V) = \int_{V_0}^{V} P_s dV + \int_{P_s}^{P_H} \frac{V}{\gamma} dP + E_{tr}, \quad (1)$$

$$\int_{T_s}^{T_H} C_V \, dT = \int_{P_s}^{P_H} \frac{V}{\gamma} dP, \quad (2)$$

and

$$T_s = T_0 \exp\left(\int_{V}^{V_0} \frac{\gamma}{V} \mathrm{dV}\right), \quad (3)$$

where subscripts $H$, $s$, 0, and 00 denote the Hugoniot, isentrope, zero-pressure specific volume of the high-pressure phase, and initial specific volume of fused quartz, respectively. The left-hand side of Eq. (1) represents the Hugoniot energy. In the case of shock reflection, the sum of the principal and reflected Hugoniot energy along a shock-compression path is taken into account. The first term on the right is the isentropic compression energy of the high-pressure phase, which we assume similar to stishovite. This contributes only a few percent temperature decrease even at 40 GPa. The value of $E_{tr}$ corresponding to the transition of fused quartz to stishovite is 0.68 MJ/kg.[15] The specific heat at constant volume is based on a Debye model, assuming a Debye temperature of 1120 K, which is appropriate for stishovite at normal conditions.[16] Recent Hugoniot data for fused quartz[4] suggest that permanent densification of the glass occurs in the region from 9 to 21 GPa, and transition to stishovite begins at 21 GPa. Since the permanent densification will tend to decrease the relative magnitude of the compressional energy term to the Hugoniot energy term by reducing the zero-pressure volume, a higher temperature ($\sim 10\%$) would result by neglecting the first and third term in Eq. (1) below 21 GPa. The shock temperature measurement for fused quartz by a radiance spectrum technique yields a value of 3600 $\pm$ 100 K at 40 GPa[17] and is in reasonable agreement with this calculation.

## III. RESULTS

Typical profiles of voltage versus time, corresponding to electrical resistivity changes during shock-wave transit are shown in Fig. 2. In Fig. 2 (b), Point 1 indicates the arrival of the shock front at the boundary between the specimen and the backing electrode, at which point the specimen is uniformly compressed. Point 1′ indicates the time when the shock wave arrives at the delay buffer plate-specimen boundary. The time interval from the onset of the oscilloscope sweep (triggered by the arrival of the shock at the interface between the target driver and delay buffer plates) to Point 1 is 0.52 $\mu$sec as compared to 0.51 $\mu$sec, which is calculated from the known shock-wave equation of state of copper and fused quartz, and the appropriate geometry. Point 2 marks the arrival of the reflected shock wave at the delay buffer plate. At Point 3 the rarefaction wave from the back surface of specimen arrives at the delay plate. As indicated in Table I, the initial shock reduces the specimen resistivity to 8.6 $\Omega$ m, whereas the reflected shock reduces the resistivity to 0.32 $\Omega$ m.

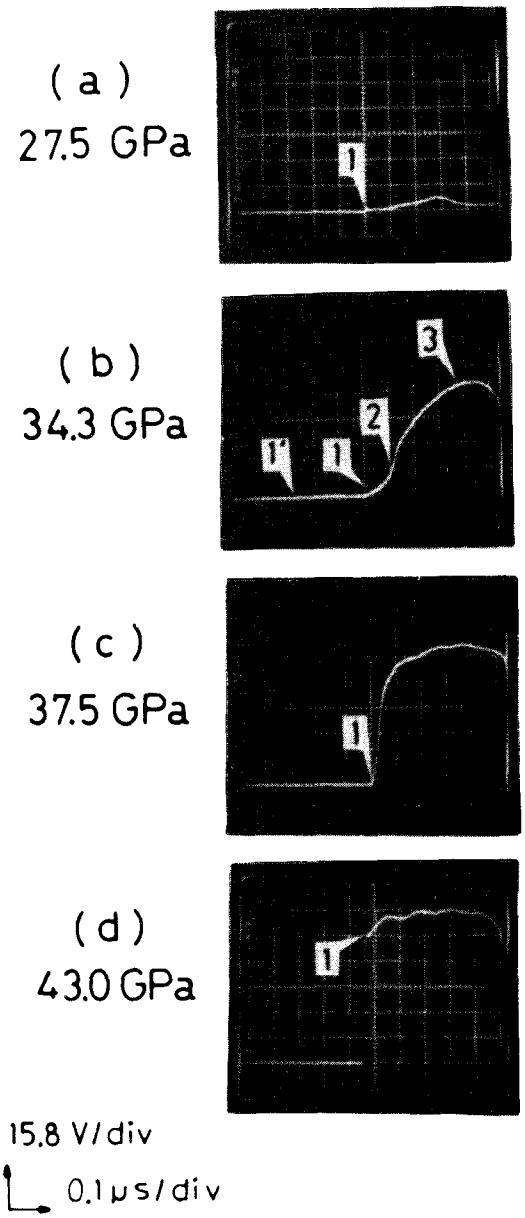


FIG. 2. Typical profiles of voltage-time corresponding to electrical resistivity changes by shock compression. Point 1′ and 1 indicate the shock arrival time at the delay plate specimen and the specimen electrode interfaces, respectively. Point 2 indicates the arrival time of the reverberated shock from the backing electrode at the specimen-delay plate interface. Point 3 indicates the time of rarefaction wave penetration from the flyer plate to the specimen. (a) shot number A-16, (b) A-25, (c) A-24, and (d) A-15.

Although the signal of Fig. 2(a) resembles the shape of 2(b), the profiles of Figs. 2(c) and 2(d) are considerably different from the others. Both voltage signals rise up to a saturating level as soon as the first shock front arrives at the sample-backing electrode boundary. The signal rise time shown in Fig. 2(c) is about 60 nsec as compared to 15 nsec in Fig. 2(d). Since the voltage changes were too small to be detected in the A-10 and A-4 experiments, the lowest limits of resistivity at the pressures were estimated by assuming that the voltage change was less than 1/20 of one division in the ordinate. Resistivity measurements are summarized in Table I and Fig. 3. It is clearly seen from Fig. 3 that the resistivity of fused quartz under shock loading gradually decreases with the first shock pressure up to 36 GPa and rapidly decreases by about two orders of magnitude at 36–40 GPa. Results of the reflected shock-compression state also show that the rapid decrease of resistivity occurs at around 70 GPa.

Polarization signals at pressures below 34.3 GPa were too small and were poorly recorded. Only three results were available and are shown in Fig. 4. Points 1, 2, and 3 in Fig. 4 correspond to the same states as Fig. 2. The signals in Fig. 4 suggest three regimes exist which qualitatively describe the electrical properties of Shock-compressed fused quartz. Figure 4(a) shows that the polarization signals are very small in both the first and reflected shock states, whereas Fig. 4(b) shows that a large negative voltage is generated upon arrival of shock front at the backing electrode. In Fig. 4(c), it is seen that a positive voltage is gradually generated following shock propagation, and that the sign of the voltage changes upon a reflection of the shock wave. Figures 4(b) and 4(c) also

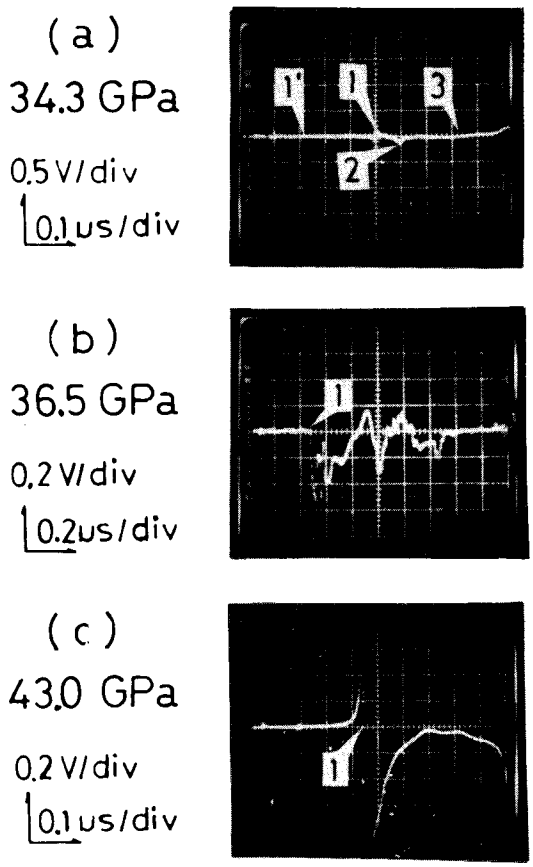


FIG. 4. Typical profiles of voltage time due to shock-induced polarization. Notation numbers of points on the photographs correspond to those in Fig. 2. (a) shot number A-25, (b) A-13, and (c) A-15.

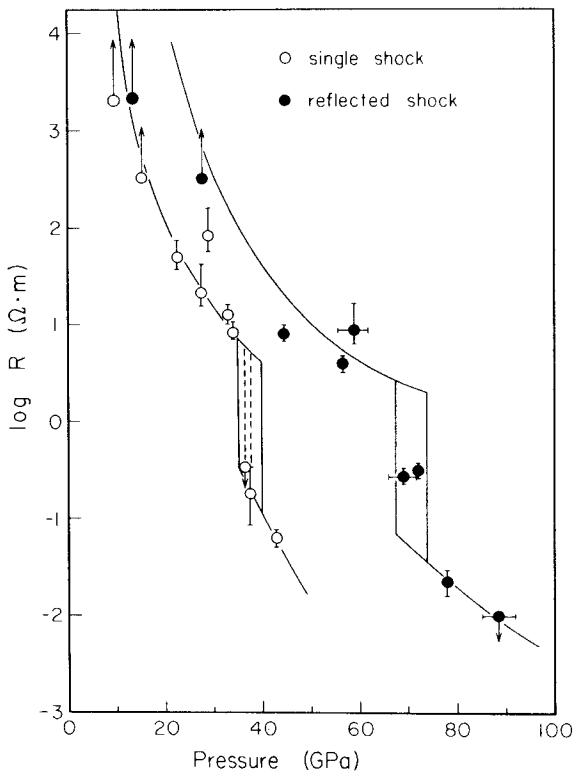


FIG. 3. Logarithm of electrical resistivity $R$ as a function of shock pressure for fused quartz.

demonstrate that the sign of the signal is positive in the direction of shock propagation, and that the response time of the polarization upon reflection of the shock wave is less than 10 nsec. The polarization signal suggests that an effective positive charge is produced at the shock front as the conductivity suddenly increases.

Since both of the electrical resistivity profiles in shot A-13 (36.5 GPa) and A-24 (37.5 GPa) are quite similar, the polarization profile of A-24 is probably similar to that in Fig. 4(b) (shot A-13). At this pressure, the rise time of the resistivity profile is longer than that of A-15 (43.0 GPa). On the other hand, when the shock-induced polarization voltage is generated following shock transit through the sample [Fig. 4(c)], the electrical conductivity signal rapidly rises [Fig. 2(d)]. This suggests that changes of the electrical properties at shock pressures of 36.5–37.5 GPa depend on time, and that the true transition in the electrical state of fused quartz occurs nearer 40 GPa and 3250 K. Although the resistivity observed for the reflected shock state for shot A-25 (72 GPa and 3500 K), where the pressure and temperature are higher than the above conditions, is of same order of magnitude as that of the first shock state for shot A-24 (37.5 GPa), the polarization signal in the reflected state is quite small. This suggests that this reflected state is in the middle of the transition in electrical properties of $SiO_2$, as shown in Fig. 3.

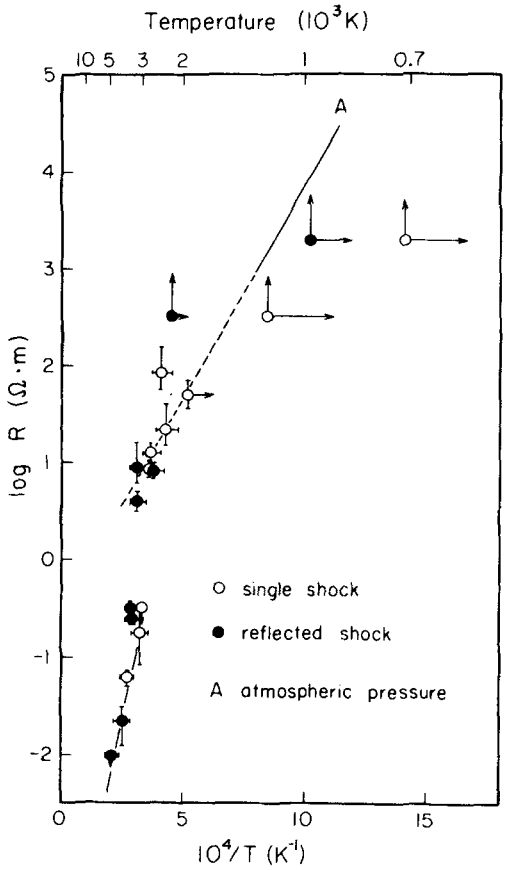


FIG. 5. Logarithm of electrical resistivity $R$ as a function of reciprocal shock temperature for fused quartz. Solid line A shows temperature dependence of resistivity for fused quartz (Ref. 29).

## IV. DISCUSSION

Molecular orbital calculations on the electronic structure of fused or amorphous quartz have been carried out using a variety of cluster models and show that the width of valence band and energy gap are of the order of 9 and ~13 eV, respectively, while the experimental value of the gap is 11 eV.[18–20] The defect electronic states are due to oxygen vacancies and proton interstitials. The latter and $Na^+$ are the main impurities in commercial fused quartz. These give rise to electron levels in the gap which are dependent on the model cluster size.[20] The oxygen vacancy is responsible for some of the ultraviolet absorption bands. The first direct measurement of the drift velocity of excess electrons in amorphous $SiO_2$ have been performed by Hughes[21] using a transit-time technique. The drift mobility was found to be $(2.0 \pm 0.3) \times 10^{-3}$ $m^2/V$ sec at 300 K, and it decreases with increasing temperature. A free electron in amorphous $SiO_2$ has a 14-nsec lifetime and a mean free path of about 4 nm. It seems that the mobility is too high to be explained by a polaron mechanism. The mobility of the holes is very low, about $4 \times 10^{-13}$ $m^2/V$ sec at 300 K, but the mean hole lifetime is over 10 sec.[22] The temperature dependence of the hole mobility is

$$2 \times 10^{-3} \exp(-0.6/kT)\ m^2/V\ \text{sec} \quad (kT \text{ in eV}). \quad (4)$$

However, the temperature dependence of the dielectric loss factor for fused quartz at low frequency is very large.[23] This corresponds to increases in ion jump frequency, dipole relaxation energy, and dc conductivity losses. Therefore, at ambient pressure and high temperature, the conduction mechanism in fused quartz may be due to ionic mobility. The diffusion coefficient for oxygen in vitreous $SiO_2$ has been measured up to 1300 K,[24,25]

TABLE I. Summary of electrical resistivity measurements under shock compression.

| Shot number (–) | Sample diameter (mm) | Sample thickness (mm) | Flyer plate (mm) | Flyer velocity (mm/μs) | Shock pressure (GPa) | Observed voltage (V) | Specific resistivity (Ω m) | Shock temperature (K) | Remarks |
|---|---|---|---|---|---|---|---|---|---|
| A-10 | 7.3 | 1.62 | Cu, 3.0 | 1.11 ± 0.01 | 9.5 ± 0.2 | < 0.01 | $> 2.0 \times 10^3$ | 710 | (a) |
| | | | | | 13.3 ± 0.3 | < 0.01 | | 980 | (b) |
| A-4 | 7.3 | 1.60 | Cu, 1.5 | 1.87 ± 0.01 | 15.2 ± 0.2 | < 0.2 | $> 3.3 \times 10^2$ | 1180 | (a) |
| | | | | | 27.7 ± 0.5 | < 0.2 | | 2160 | (b) |
| A-11 | 7.3 | 1.62 | Cu, 1.5 | 2.59 ± 0.01 | 22.5 ± 0.2 | 0.6 ± 0.2 | $4.9 \times 10^1$ | 1920 | (a) |
| | | | | | 44.5 ± 0.5 | 1.2 ± 0.2 | 8.1 | 2620 | (b) |
| A-16 | 7.3 | 1.59 | Cu, 1.5 | 3.01 ± 0.05 | 27.5 ± 1.0 | 1.5 ± 0.7 | $2.2 \times 10^1$ | 2300 | (a) |
| | | | | | 56.5 ± 1.0 | 3.1 ± 0.7 | 4.0 | 3180 | (b) |
| A-20 | 7.3 | 1.65 | W, 0.8 | 2.43 ± 0.05 | 29.0 ± 1.0 | 0.4 ± 0.2 | $8.4 \times 10^1$ | 2420 | (a) |
| | | | | | 59.0 ± 3.0 | 1.3 ± 0.6 | 9.1 | 3250 | (b) |
| A-21 | 7.3 | 1.59 | W, 0.8 | 2.72 ± 0.05 | 33.0 ± 1.0 | 2.7 ± 0.6 | $1.3 \times 10^1$ | 2680 | (a) |
| | | | | | 69.0 ± 3.0 | 32 ± 4 | $2.7 \times 10^{-1}$ | 3430 | (b) |
| A-25 | 7.3 | 1.59 | W, 0.8 | 2.80 ± 0.01 | 34.3 ± 0.2 | 3.9 ± 0.8 | 8.6 | 2760 | (a) |
| | | | | | 72.0 ± 0.4 | 29 ± 3 | $3.2 \times 10^{-1}$ | 3500 | (b) |
| A-13 | 5.8 | 1.33 | W, 0.8 | 2.87 ± 0.01 | 36.5 ± 0.2 | > 40 | $< 3.3 \times 10^{-1}$ | 2970 | (a) |
| | | | | | 75.5 ± 0.5 | ... | ... | 3740 | (b) |
| A-24 | 7.3 | 1.65 | W, 0.8 | 2.94 ± 0.01 | 37.5 ± 0.2 | 61 ± 13 | $1.8 \times 10^{-1}$ | 3070 | (a) |
| | | | | | 78.0 ± 0.5 | 78 ± 4 | $2.2 \times 10^{-2}$ | 3880 | (b) |
| A-15 | 7.3 | 1.57 | W, 0.8 | 3.20 ± 0.05 | 43.0 ± 1.2 | 78 ± 2 | $6.2 \times 10^{-2}$ | 3650 | (a) |
| | | | | | 88.5 ± 3.5 | 90 ± 2 | $1 \times 10^{-2}$ | 4710 | (b) |

[a]First shock state.
[b]Reverberated state.

TABLE II. Summary of shock-induced polarization experiments.

| Shot number (−) | Sample diameter (mm) | Sample thickness (mm) | Flyer plate (mm) | Flyer velocity (mm/μs) | Shock pressure (GPa) | Maximum voltage (V) | Characterized[a] polarization (V/m) | Shock temperature (K) | Remarks |
|---|---|---|---|---|---|---|---|---|---|
| A-25 | 7.3 | 1.59 | W, 0.8 | 2.80 ± 0.01 | 34.3 ± 0.2 | + 0.1 | 6.4 | 2760 | b |
| | | | | | 72.0 ± 0.4 | − 0.2 | $1.2\times10^{1}$ | 3500 | c |
| A-13 | 5.8 | 1.33 | W, 0.8 | 2.87 ± 0.01 | 36.5 ± 0.2 | ... | ... | 2970 | b |
| | | | | | 75.5 ± 0.5 | − 0.6 | $5.2\times10^{1}$ | 3740 | c |
| A-15 | 7.3 | 1.57 | W, 0.8 | 3.20 ± 0.05 | 43.0 ± 1.2 | > + 0.6 | $3.7\times10^{1}$ | 3650 | b |
| | | | | | 88.5 ± 3.5 | < − 1.0 | $5.7\times10^{1}$ | 4710 | c |

[a]Characterized polarization is defined as proportion to length and inverse proportion to area, and its sign is positive for shock propagating direction.
[b]First shock state.
[c]Reverberated state.

$$2.88 \times 10^{-8} \exp(-1.17/kT)\ \mathrm{m^2/sec}\ (kT \text{ in eV}). \quad (5)$$

The diffusion coefficients for oxygen and silicon in silicates have been recently measured.[26,27] Since the mobility of $Si^{+4}$ is apparently comparable to that of $O^{2-}$, both species could possibly contribute to ionic conductivity. A molecular dynamic simulation for fused quartz by Woodcook *et al.*[28] suggests that both the self-diffusion coefficients for oxygen and silicon ions have similar values at very high temperatures.

The resistivity versus reciprocal shock temperature (Fig. 5) clearly demonstrates two regimes of electrical resistivity behavior. The temperature dependence of resistivity for fused quartz at atmospheric pressure has been reported[29] and is also shown in Fig. 5. This is approximately represented by the equation

$$R = 0.251 \exp(0.88/kT), \quad (6)$$

where $R$ and $kT$ are in $\Omega$·m and eV, respectively. An extrapolation of this line agrees well with shock-wave data with larger resistivity than 1 $\Omega$·m. In the regime over which the high-temperature and high-pressure data agree, we believe that fused quartz has partially transformed to stishovite. Therefore, we infer no significant difference exists between ionic transport processes in normal fused quartz and the presumed shock-induced high-pressure phase, stishovite.

However, at the higher temperature, the effective activation energy suddenly changes and the resistivity is approximately represented as

$$R = 2 \times 10^{-5} \exp(2.4 \pm 0.5/kT), \quad (7)$$

where the results of the reflected shock state in shots A-25 and A-21 are regarded as in the transition state. This sudden change of activation energy suggests an occurrence of structural change in silica at high temperature and high pressure.

Two possibilities can be considered to explain the transition: One is that a six-coordinated glass still exists[6] and gives rise to glass transition or crystallization above that pressure and temperature. The second possibility is due to unknown phase transition, e.g., stishovite to another solid or stishovite to liquid. Molecular dynamic simulations suggest that a high-density glass can exist at such high pressure.[28] That the electrical transition temperature observed here appears not to depend strongly on pressure is consistent with the glass-transition behavior.[28,29] Moreover, a lack of a pressure effect on the activation energy suggests that fused quartz remains a glass up to the transition pressure. If this is the case, the calculated temperature should be increased by setting the $E_{tr}$ term in Eq. (1) to zero. This will provide closer agreement with the present calculation and observed shock temperature at 40 GPa.[17] Supporting the second hypothesis, Liu *et al.* have found a new modification of $SiO_2$ with similar density of stishovite by using a diamond anvils technique.[31] German *et al.* have also found a polymorph of $SiO_2$ which is 2.4% denser than stishovite by a shock-recovery method.[32,33] Although these phases may only have high-pressure-temperature stability fields, the possibility of yet another high-pressure structure for $SiO_2$ cannot be ruled out. The existing pressure-density Hugoniot data do not show an anomalous density change associated with this transition.

Although a resistivity decrease of about two orders of magnitude occurs on melting in some minerals,[34,35] this does not appear to be consistent with the shock temperature measurements for fused quartz,[36,37] which suggest that the onset of melting of stishovite under shock loading occurs at a higher pressure and temperature than the ~40 GPa and ~3300 K observed for the change in electrical conductivity. However, in the shock temperature measurement by using a radiance spectrum technique, the experimental results of Lyzenga and Ahrens[36,37] suggest that the light originates in a thin layer near or coincident with the shock front. The extremely short (< 5 nsec) rise and decay times in these experiments would not be observed, if the radiance source were distributed throughout a large volume of the sample. Therefore, it is possible to interpret their results as superheating of $SiO_2$ above the melting temperature, if the final state takes longer than the shock front to equilibrate. On the other hand, the electrical conductivity measurement is sensitive to the properties of the entire sample volume. Thus both experiments may, in fact, be detecting shock-induced melting. The pressure and temperature states observed for the sudden change in electrical conductivity may correspond to the onset of the superheated regime of Lyzenga and Ahrens, and hence may define a point on the melting line of stishovite.[36–38] It has, however, been reported that the electrical conductivity of natural single-crystal albite ($NaAlSi_3O_8$) increases by about $10^4$ at a temperature close to the melting point at high temperatures and controlled oxygen fugacity.[39] The results suggest that the actual onset of melting need not

be invoked to explain large changes in resistivity. The possible effects of heterogeneity during shock compression might promote this mechanism. However, it is unclear what the mechanism for conduction of albite actually is and if the mechanism is applicable to conduction in shocked $SiO_2$.

## ACKNOWLEDGMENTS

The authors appreciate the interest and encouragement proffered by Y. Syono of Tohoku University in carrying out this research. The work was partially supported under the Japan-U.S. Cooperative Science Program: Y. Syono and T. J. Ahrens are grateful for the support from the Japan Society for the Promotion of Science (grant 4R032) and U. S. National Science Foundation (grant DES 75-15006 and FJ4035). Contribution No. 3565, Division of Geological and Planetary Sciences, California Institute of Technology, Pasadena, California 91125.

[1]J. Wackerle, J. Appl. Phys. **33**, 922 (1962).
[2]L. V. Al'tshuler, R. F. Trunin, and G. V. Simakov, Izv. Acad. Sci. USSR, Phys. Solid Earth **10**, 657 (1965).
[3]R. F. Trunin, G. V. Simakov, and M. A. Podurets, Izv. Acad. Sci. USSR, Phys. Solid Earth **2**, 102 (1971).
[4]H. Sugiura, K. Kondo, and A. Sawaoka, J. Appl. Phys. **52**, 3375 (1981).
[5]R. A. Graham, F. W. Neilson, and W. B. Benedick, J. Appl. Phys. **36**, 1775 (1965).
[6]R. G. McQueen, J. N. Fritz, and S. P. Marsh, J. Geophys. Res. **68**, 2319 (1963).
[7]J. D. Kleeman and T. J. Ahrens, J. Geophys. Res. **78**, 5954 (1973).
[8]D. E. Grady, W. J. Murri, and G. R. Fowles, J. Geophys. Res. **79**, 332 (1974).
[9]K. Kondo, A. Sawaoka, and S. Saito, Rev. Sci. Instrum. **48**, 1581 (1977).
[10]R. K. Linde and D. N. Schmidt, Rev. Sci. Instrum. **37**, 1 (1966).
[11]T. J. Ahrens, J. Appl. Phys. **37**, 2532 (1966).
[12]K. Kondo, T. Mashimo, and A. Sawaoka, J. Geophys. Res. **85**, 977 (1980).
[13]T. Mashimo, K. Kondo, A. Sawaoka, Y. Shyono, H. Takei, and T. J. Ahrens, J. Geophys. Res. **85**, 1876 (1980).
[14]R. G. McQueen, S. P. Marsh, J. W. Taylor, J. N. Fritz, and W. J. Carter, *High Velocity Impact Phenomena*, edited by R. Kinslow (Academic, New York, 1970), p. 244.
[15]R. A. Robie, B. S. Hemingway, and J. R. Fisher, *Thermodynamic Properties of Minerals and Related Substances at* 298.15*K and* 1 *Bar* ($10^5$ *Pascals*) *Pressure and at Higher Temperatures*, (Government Printing Office, Washington, D.C., 1978), pp 216.
[16]G. F. Davies, J. Geophys. Res. **77**, 4920 (1972).
[17]H. Sugiura, K. Kondo, and A. Sawaoka, Rev. Sci. Instrum. **51**, 750 (1980).
[18]K. L. Yip and W. B. Fowler, Phys. Rev. B **10**, 1400 (1974).
[19]A. G. Revesz, Phys. Rev. Lett. **27**, 1578 (1971).
[20]A. J. Bennett and L. M. Roth, J. Phys. Chem. Solids **32**, 1251 (1971).
[21]R. C. Hughes, Phys. Rev. Lett. **30**, 1333 (1973).
[22]R. C. Hughes, Appl. Phys. Lett. **26**, 436 (1975).
[23]W. D. Kingery, H. K. Bowen, and D. R. Uhlmann, *Introduction to Ceramics*, 2nd ed. (Wiley, New York, 1976), p. 939.
[24]F. J. Norton, Nature (London) **191**, 701 (1961).
[25]R. L. Meek, J. Am. Ceram. Soc. **56**, 341 (1973).
[26]K. P. R. Reddy, S. M. Oh, L. D. Major, Jr., and A. R. Cooper, J. Geophys. Res. **85**, 322 (1980).
[27]O. Jaoul, C. Forideveax, and M. Poumellec, (abstract) IUGG XVII General Assembly, Canberra, Australia (1979).
[28]L. V. Woodcock, C. A. Angell, and P. Cheeseman, J. Chem. Phys. **65**, 1565 (1976).
[29]R. W. Wallace and E. Ruh, J. Am. Ceram. Soc. **50**, 358 (1967).
[30]R. D. Maurer, J. Am. Ceram. Soc. **40**, 211 (1957).
[31]L. Liu, W. A. Bassett, and J. Sharry, J. Geophys. Res. **83**, 2301 (1978).
[32]V. N. German, M. A. Produrets, and R. F. Trunin, Sov. Phys. JETP **37**, 107 (1973).
[33]V. N. German, N. N. Orlova, L. A. Tarasova, and R. F. Trunin, Izv. Acad. Sci. USSR, Phys. Solid Earth **11**, 431 (1975).
[34]T. Murase and A. R. McBirney, Geol. Soc. Am. Bull. **84**, 3563 (1973).
[35]T. J. Shankland, Rev. Geophys. Space Phys. **17**, 792 (1979).
[36]G. A. Lyzenga and T. J. Ahrens, Geophys. Res. Lett. **7**, 141 (1980).
[37]G. A. Lyzenga and T. J. Ahrens (unpublished).
[38]K. Kondo and A. Sawaoka, (abstract) HPC XX, in Japanese, Kobe, Japan (1979).
[39]A. J. Piwinskii and A. Duba, Geophys. Res. Lett. **1**, 209 (1974).